Journal of
Ceramic Science
and Technology

J. Ceram. Sci. Technol., **09** [1] 37-42 (2018)
DOI: 10.4416/JCST2017-00056
available online at: http://www.ceramic-science.com

Manufacturing of SiO_2-Coated β-TCP Structures by 3D Printing using a Preceramic Polymer as Printing Binder and Silica Source

R. de Melo Bernardino[1], C. Wirth[2], S.L. Stares[3], G.V. Salmoria[1], D. Hotza[*2], J. Günster[4]

[1]Laboratory of Innovation on Additive Manufacturing and Molding (NIMMA), Federal University of Santa Catarina (UFSC), 88040 – 900 Florianópolis, SC, Brazil
[2]Siemens AG, Huttenstr. 12, D-10553 Berlin, Germany
[3]Interdisciplinary Laboratory for the Development of Nanostructures (LINDEN), Federal University of Santa Catarina (UFSC), 88040 – 900 Florianópolis, SC, Brazil
[4]Federal Institute for Materials Research and Testing (BAM), Ceramic Processing and Biomaterials, D-12203 Berlin, Germany

received July 16, 2017; received in revised form September 20, 2017; accepted October 10, 2017

Abstract

Tricalcium phosphate (β-TCP) can be used as bone graft, exhibiting suitable bioabsorption and osteoconduction properties. The presence of silica may induce the formation of a hydroxyapatite layer, enhancing the integration between implant and bone tissue. Preceramic polymers present silicon in their composition, being a source of SiO_2 after thermal treatment. Using the versatility of 3D printing, β-TCP and a polysiloxane were combined to manufacture a bulk β-TCP with a silica coating. For the additive manufacturing process, PMMA powder was used as passive binder for the β-TCP particles, and polymethylsilsesquioxane (MK), dissolved in an organic solvent, was used both as a printing binder (ink) and as the source of SiO_2 for the coating. Five distinct coating compositions were printed with increasing amounts of MK. The structures were then submitted to heat treatment at 1180 °C for 4 h. XRD and FTIR showed no chemical reaction between the calcium phosphate and silica. SEM allowed observation of a silicon-based coating on the structure surface. Mechanical strength of the sintered porous structures was within the range of that of trabecular bones.

Keywords: Tricalcium phosphate, three-dimensional printing, preceramic polymer, bone regeneration

I. Introduction

Because of their similarity to the mineral part of bone, bioceramics such as calcium phosphate have been applied to promote the regeneration of bone tissue, especially hydroxyapatite and tricalcium phosphate. Among these bioceramics, hydroxyapatite is the most commonly applied as dental material or orthopedic graft. However, hydroxyapatite grafts may remain in the body for years after implantation, hindering total bone regeneration [1]. Tricalcium phosphate also has important biological properties, such as osteoconduction. As a bioceramic, β-TCP, which is the phase of tricalcium phosphate stable at temperatures up to 1180 °C [2], is absorbable by the organism, in compatible rates with the process of new bone formation, which may lead to complete bone regeneration [3]. The use of artificial grafts for bone regeneration is restricted not only to bioceramics. Bioglasses, for example, have silica (SiO_2) in their composition and are biocompatible. The presence of silica might help to promote the growth of a hydroxyapatite layer on the surface, making possible a totalintegration between implant and bone tissue. However, bioglasses show low values of mechanical strength and a high absorption time [4].

In addition to bioceramics and bioglasses, the use of preceramic polymers (PCPs) to manufacture bone grafts is an option in tissue engineering applications [5,6]. PCPs have a main chain formed by silicon (Si) that, after a suitable thermal treatment, may convert into a ceramic material, known as Polymer-Derived Ceramic or PDC. Yielded PDCs might be silica (SiO_2), silicon oxide carbide (SiOC) or silicon carbide (SiC), depending on the polymeric precursor and heat treatment [7,8]. An example of preceramic polymer is polymethylsilsesquioxane [9]. Using PCPs takes advantage of fabrication processes normally associated with polymeric materials to produce ceramic products [10]. Ceramic materials need high temperatures during their manufacturing process. This is essential for the materials to reach desired mechanical properties. However, sintering can result in high porosity, volumetric shrinkage and cracks in the final product. Polymeric materials have rheological properties that change with the temperature. This property enables the manufacturing of products using processes with varying temperature and pressure, where the material is heated to improve its fluidity and is forced against a mold. The versatility of shapes and geometries of

* Corresponding author: d.hotza@ufsc.br

polymeric products that can be produced in a process like injection may lead to high productivity [11]. A broad range of new designs and applications of PCPs is opened up by Additive Manufacturing (AM) techniques, which allow the fabrication of ceramic components with complex geometry and composition [12].

3D Printing (3DP) is an AM process that deposits a binder material layer by layer onto a powder bed with the help of inkjet printer heads. The processes can be employed to fabricate a wide variety of shapes with tailored macro- and microscopic porosities for many applications [13–15]. Other works have shown that it is possible to produce ceramics by means of 3DP from a preceramic polymer [8–9], but in these cases the PCP was mixed with the powder bed. In the present research, a novel possibility for obtaining porous structures has been developed. The goal was to produce porous composite structures by means of 3DP with different SiO_2 contents from a preceramic polymer used as a printing ink and β-TCP as the powder bed.

II. Experimental

(1) Materials

The 3DP process generally requires a solid material laid in a powder bed and a liquid ink to be dropped on the powder by a printing cartridge, acting as a powder binder. In the present work, a blend of two powders was used as solid material and two liquids were respectively employed as a printing ink.

The powders were a mix of β-TCP, with a mean particle size of 35 µm, synthesized at BAM (Bundesanstalt für Materialforschung und -prüfung, Berlin, Germany), and commercially available polymethylmethacrylate (PMMA, Voxeljet, Friedberg, Germany) with average particle size of 72 µm, acting as an auxiliary binder. These powders were mixed in a mechanical mixer for a period of 6 h at 32 rpm. PMMA content in the powder mix was 20 wt% (Hausner Ratio = 1.46) [16].

The liquids employed were Polypor B (1-hexanol hexyl acetate, Voxeljet, Friedberg, Germany), used as a solvent, and a commercial PCP, polymethylsilsesquioxane (MK, Wacker, Burghausen, Germany), previously dissolved in Polypor B, used as a binder and source of silica.

(2) Additive manufacturing

To fabricate the samples, a tridimensional printer was used (3D Voxeljet Teststand VTS 16, Friedberg, Germany) with two printing cartridges (SM-128 AA, Fujifilm), respectively named P1 (solvent Polypor B) and P2 (preceramic polymer MK). These are piezoelectric cartridges with 128 nozzles, each with a diameter of 508 µm. Produced specimens are discs with 15 mm diameter × 4.5 mm thickness, each consisting of 30 deposited 150-µm layers. The total saturation values for the solvent (cartridge P1) were 0.25 $g \cdot cm^{-3}$ and 0.021 $g \cdot cm^{-3}$ for PCP binder (cartridge P2). The 3D printer used enables the repetition of the printer steps over the same layer with more applications of the MK-containing cartridge P2, making it possible to increase the final amount of yielded SiO_2 after thermal treatment, as shown in Table 1.

Table 1: Printed groups with increasing yielded SiO_2.

Group	Number of repetitions of cartridge P2	SiO_2 (wt%) yield after heat treatment
1	0	0
2	1	0.25
3	3	0.75
4	5	1.25
5	10	2.50

The specimens were thermally treated in air atmosphere in an electrically heated furnace (HT 16/17, Nabertherm, Lilienthal, Germany). A single-step annealing sequence was applied, where the temperature was raised with a constant heating rate of 10 K/min^{-1} up to 200 °C, followed by a heating rate of 5 K/min^{-1} up to 1180 °C. The specimens were sintered at 1180 °C for 4 h and cooling was set to 10 K/min^{-1} [2,17].

(3) Microstructural, physical and mechanical characterization

X-ray diffraction (XRD) profiles of the sintered porous structures were recorded by means of powder diffractometry (PW1710 Philips, Holland) using monochromatic Cu-Ka radiation with a scan rate of $1° \cdot min^{-1}$ over a 2θ range of 10–70°. IR spectra of sintered porous structures were obtained using a Fourier-Transform Infrared spectrometer (FTIR Perkin Elmer, Waltham, USA) along a band of 1400–400 cm^{-1} with 0.5 cm^{-1} resolution. Micrographs from the surface of porous structures were obtained by means of SEM (Supra 40 Carl Zeiss AG, Oberkochen, Germany) coupled with an EDS system.

The apparent density of the specimens (ϱ_{ap}) was determined from weight and volume measurements. Skeletal density ($\varrho_{skeletal}$) was measured by means of pycnometry (Pycnomatic ATC, Thermo Fisher, Waltham, USA). Total porosity (ϱ_p) was derived from fractional densities ϱ^* according to Equation 1

$$\rho_p = 1 - \rho^* = \frac{1 - \rho_{ap}}{\rho_{skeletal}} \quad (1)$$

The mechanical strength of the sintered porous structures was measured using the ball-on-three-balls (B3B) test, which permits testing of thin as-sintered specimens [18]. A constant crosshead speed of 2 $mm \cdot s^{-1}$ was applied in a universal test machine (Zwick/Roell, Ulm, Germany).

III. Results and Discussions

Fig. 1 shows XRD patterns of sintered porous structures, indicating no reactions between the calcium phosphate and silicon oxide. This may have happened owing to the small quantities of SiO_2 in the specimens, even in the case of maximum 2.5 wt%. Another factor that could be responsible for the absence of reactions was the amorphous nature of SiO_2 after sintering. In a previous work, amorphous silica was also detected for the preceramic polymer MK after the same heating profile [19].

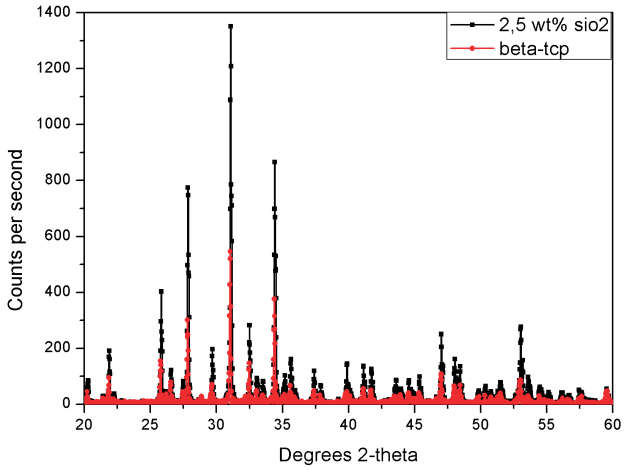

Fig. 1: XRD patterns of sintered β-TCP porous structures with (black) or without (red) 2.5 wt% SiO_2.

Fig. 2 shows the FTIR spectra of sintered porous structures. In Curve 1 (black) for pure β-TCP, it is possible to notice a large band between 900 and 1100 cm^{-1} corresponding to the overlap of PO_4^{-3} stretching modes. The peaks close to 600 cm^{-1} and 540 cm^{-1} correspond to the vibration of PO_4^{-3}, indicating the presence of β-TCP [20]. Curves 2 and 3, red and blue respectively, show increasing SiO_2 content. The growth of a peak near 450 cm^{-1} is related to stretching vibrations of Si-O-Si [21]. Moreover, two regions are also observed with regard to the Si-O bond: around 800 cm^{-1} and 1240 cm^{-1}. The absence of a peak near 740 cm^{-1} is evidence that there was no reaction between silicon and carbon during the conversion of PCP [22].

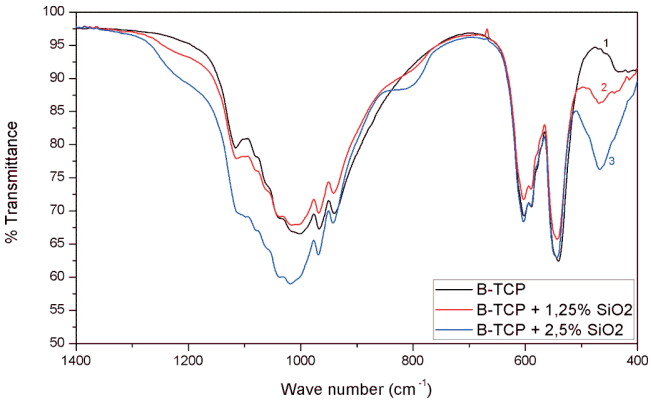

Fig. 2: FTIR spectra of sintered porous structures β-TCP with increasing SiO_2 contents.

From SEM micrographs, the morphology of printed parts after sintering was verified. The analyses were determinant in identifying SiO_2 after printing, owing to the presence of Si-rich material on the particles of β-TCP. Fig. 3a shows an image of the surface where large void regions with semi-spherical format are observed, where possibly PMMA particles were present. The average pore size was 40 µm. In Fig. 3b (0.25 wt% SiO_2), two different points were identified, pt1 and pt2. Fig. 3c shows that in pt1 it was possible to identify the elements calcium, phosphorus, oxygen and silicon. In pt2 the element silicon was not detected. The carbon in both spectra comes from the conductive coating applied to the surface for SEM analysis. Fig. 3d shows details of the SiO_2 coating on the β-TCP surface.

Burnout of the polymeric phase as well as the nature of the 3DP process itself resulted in high porosity in the sintered structures (Fig. 3a). The calculated total porosity was in the range of 63 – 70 %, since there was no high densification of the powders, as expected [23].

Fig. 4 shows the ultimate strength of sintered β-TCP porous structures as well as the total porosity as a function of the amount of yielded silica. The ultimate strength was lower than 1 MPa with a high standard deviation of 20 to 30 %. Porosity is mainly responsible for this feature, which is related to the 3DP process itself, since the powders are submitted to low compacting pressures. Moreover, the sintering process was not sufficient to cause a significant improvement in the densification of the parts. The amount of silica does not appear to have an effect on the strength of the sintered porous structures. It is possible to verify that for higher contents of SiO_2 there was a small increase of the average strength; but from 1.25 wt%, the effect of silica was negative, exhibiting values similar to the group that does not contain this material in its composition. Nevertheless, the values of mechanical resistance are consistent with those found in other similar works [19].

Pores and internal defects are responsible for low average and high dispersion of mechanical strength values in ceramic materials, so that the control of such defects over processing is essential. However, from the point of view of 3D printing, pores are intrinsically correlated with the process implementation, limiting the mechanical properties of the final parts. Although there is variation in the porosity within and between the groups, the overall picture is of a low mechanical resistance that is compatible with 3DP ceramic parts.

In tissue engineering, a number of architectural characteristics, including porosity, pore size, and permeability are significant parameters in biological delivery and tissue regeneration. The ability to control graft architecture can provide significant insights into how graft architecture and material affect tissue regeneration. Previous studies on bone grafts have found that both macro- and microporosity play an important role in osteogenesis and bone regeneration [24,25]. Structures with high porosity enable effective release of biofactors such as proteins, genes, or cells and provide good substrates for nutrient exchange. However, the mechanical behavior that is important in maintaining the structural stability of the material is often compromised as the result of increased porosity [26]. Previous works have shown that grafts with level of porosity from 40 to 65 % were able to promote the connection and proliferation of cells in biological tests [27–29]. For bone grafts, in general, pore sizes in the range of 20 – 60 µm are ideal for cell spreading and

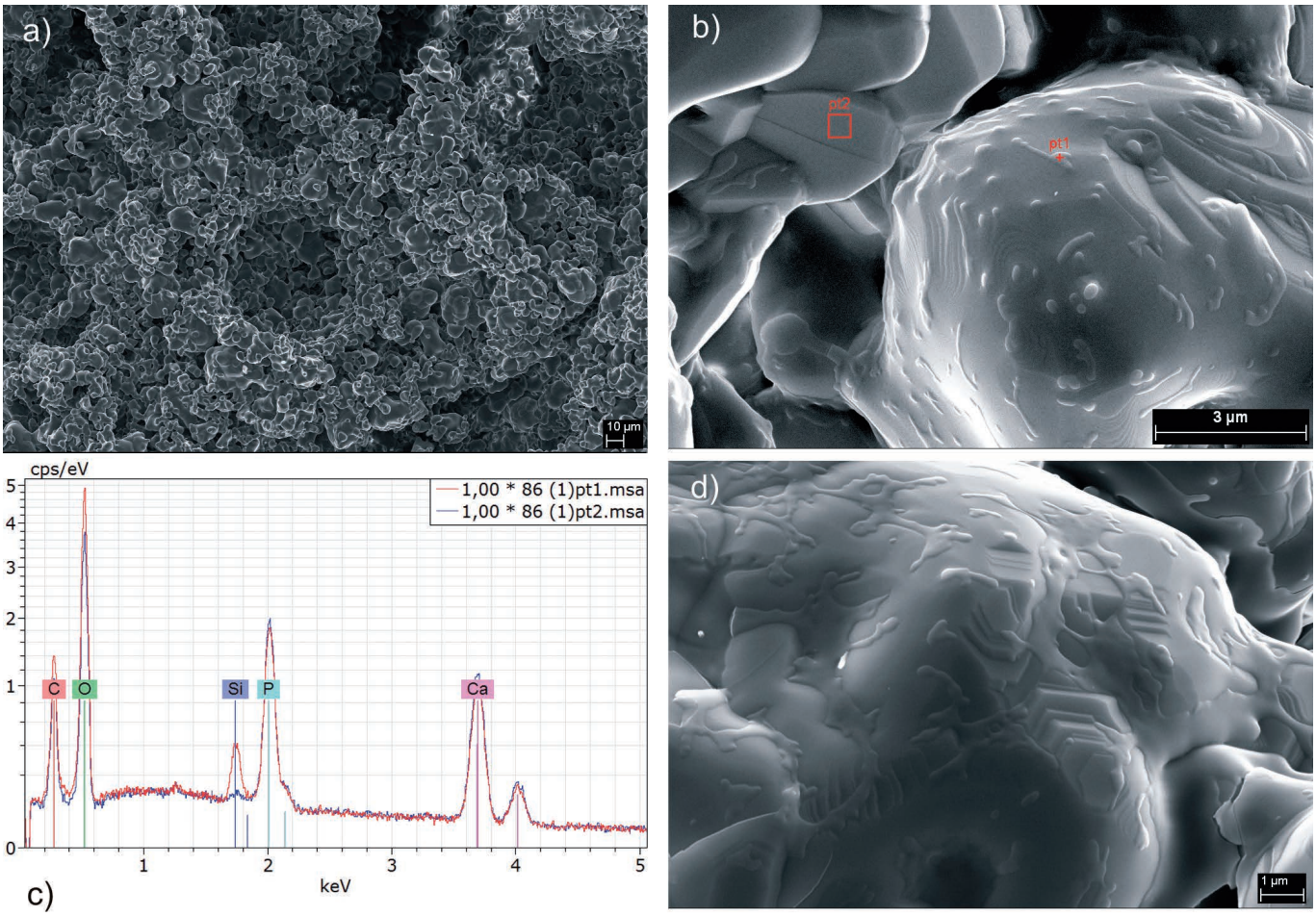

Fig. 3: Surface of sintered porous structures: a) SEM of β-TCP only; b) SEM of β-TCP + 0.75 wt% SiO_2; c) EDS of β-TCP + 0.25 wt% SiO_2; and d) SEM of β-TCP + 2.5 wt% SiO_2.

proliferation. Moreover, a minimum pore size of approximately 100 µm is considered sufficient to enable bone tissue regeneration to occur [30–32].

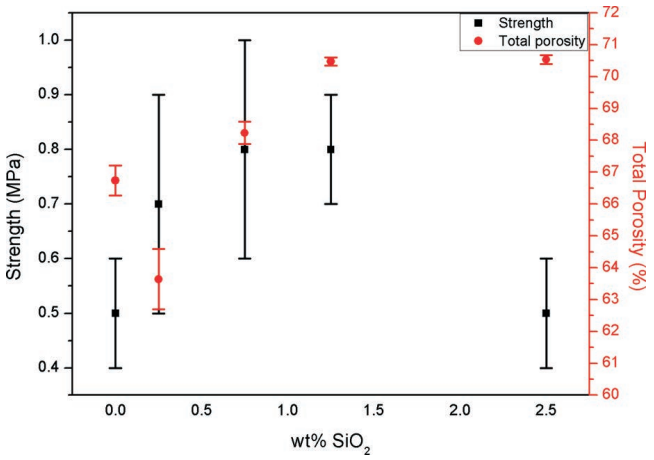

Fig. 4: Total porosity (%) and mechanical strength (MPa) of sintered β-TCP porous structures with varying amounts of yielded SiO_2 on the surface.

Regarding mechanical properties, the bone structure is dynamic in time and becomes fit to withstand any imposed stresses in an adaptive manner. The values of the mechanical properties are not constant from bone to bone, from individual to individual, and therefore, only mean data are obtained. For trabecular human bone, for example, ultimate strength values in the order of 0.1 to 16 MPa and elastic modulus values of 0.12 to 1.1 GPa have been determined depending on density and orientation [33,34]. The strength values of sintered porous structures obtained in this research are thus within the range of strength of trabecular bones, which can make them suitable for use in bone tissue engineering.

IV. Conclusions

This paper describes the development of an innovative approach for the 3DP fabrication of bioceramic composites consisting of bulk β-TCP and a partially coated SiO_2 surface, which was derived from a preceramic polymer. XRD and FTIR analysis indicated no interaction between β-TCP and PCP. Moreover, the interaction seems to be only physical, as shown by SEM and EDS analysis. After repeated depositions of MK solution, SEM/EDS revealed a second silicon-based phase formation on the surface of β-TCP particles, resembling a coating. The B3B tests showed low mechanical strength values of the sintered parts, resulting from the high porosity (63 – 70 %) caused by the PMMA binder removal and the inherent characteristics of the 3DP manufacturing, and also due to the partial sintering of β-TCP in the heat treatment conditions employed. Nevertheless, the mechanical resistance is coherent with results of similar works. In conclusion, this work

showed a new manufacturing 3DP route using a preceramic polymer directly as a printing ink, broadening the opportunities for new designs and applications, which might include composites and functionally graded materials.

References

1 Dorozhkin, S.V.: Biphasic, triphasic and multiphasic calcium orthophosphates, *Acta Biomater.,* **8**, [3], 963 – 977, (2012).

2 Pillai, R.S., Sglavo, V.M.: Effect of MgO addition on solid state synthesis and thermal behavior of beta-tricalcium phosphate, *Ceram. Int.*, **41**, [2], 2512 – 2518, (2015).

3 Horowitz, R.A., *et al.*: β-tricalcium phosphate as bone substitute material: properties and clinical applications, *J. Osseointegration*, **2**, [2], 61 – 68, (2010).

4 Hench, L.L., Thompson, I.: Twenty-first century challenges for biomaterials, *J. R. Soc. Interface*, **7**, 379 – 391, (2010).

5 Elsayed, H., *et al.*: Development of bioactive silicate-based glass-ceramics from preceramic polymer and fillers, *J. Eur. Ceram. Soc.*, **35**, [2], 731 – 739, (2015).

6 Elsayed, H., *et al.*: Hardystonite bioceramics from preceramic polymers, *J. Eur. Ceram. Soc.*, **36**, [3], 829 – 835, (2016).

7 Greil, P.: Polymer derived engineering ceramics. *Adv. Eng. Mater.*, **2**, [6], 339 – 348, (2000).

8 Sanson, O.: Preceramic polymer-derived ceramic scaffolds by 3D-printing. Universitá Degli Studi di Padova, PhD Thesis, 2014.

9 Zocca, A., *et al.*: SiOC ceramics with ordered porosity by 3D-printing of a preceramic polymer, *J. Mater. Res.*, **28**, [17], 2243 – 2252, (2013).

10 Colombo, P., *et al.*: Polymer-derived ceramics: 40 years of research and inovation in advanced ceramics, *J. Am. Ceram. Soc.*, **93**, [7], 1805 – 1837, (2010).

11 Callister, Jr, W.D., Rethwisch, D.G.: Materials science and engineering: An introduction. 9th ed. New York, Wiley, 2014.

12 Colombo, P., *et al.*: Additive manufacturing techniques for fabricating complex ceramic components from preceramic polymer, *Am. Ceram. Soc. Bull.*, **96**, [3], 16 – 23, (2016).

13 Liu, F.H.: Synthesis of biomedical composite scaffolds by laser sintering: mechanical properties and in vitro bioactivity evaluation, *Appl. Surf. Sci.*, **297**, 1 – 8, (2014).

14 Liu, F.H., Shen, Y.K., Lee, J.L.: Selective laser sintering of a hydroxyapatite-silica scaffold on cultured MG63 osteoblasts *in vitro*, *Int. J. Precis. Eng. Man.*, **13**, [3], 439 – 444, (2012).

15 Chartier, T., *et al.*: Additive manufacturing to produce complex 3D ceramic parts. *J. Ceram. Sci. Tech.*, **6**, [2], 95 – 104, (2015).

16 Carr, R.L.: Evaluating flow properties of solids. *Chem. Eng.*, **72**, [2], 163 – 168, (1965).

17 Stares, S.L., *et al.*: Paper-derived β-TCP. *Mater. Lett.*, **98**, 161 – 163, (2013).

18 Danzer, R., Supancic, P., Harrer, W.: Biaxial tensile strength test for brittle rectangular plates, *J. Ceram. Soc. Japan*, **114**, [11], 1054 – 1060, (2006).

19 Zocca, A., *et al.*: 3D-printed silicate porous bioceramics using a non-sacrificial preceramic polymer binder, *Biofabr.*, **7**, 1 – 12, (2015).

20 Ananth, K.P., Shanmugam, S., Jose, S.P., Nathanael, A.J., Oh, T.H., Mangalaraj, D., Ballamurugan, A.M.: Structural and chemical analysis of silica-doped β-TCP ceramic coating on surgical grade 316L SS for possible biomedical application, *J. Asian. Cer. Soc*, **3**, [3], 317 – 324, (2015).

21 Ma, Q., Ma, Y., Chen, Z.: Fabrication and characterization of nanoporous SiO_2 ceramics via pyrolysis of silicone resin filled with nanometer SiO_2 powders, *Ceram. Int.*, **36**, [8], 2269 – 2272, (2010).

22 Kopani, M., Mikula, M., Takahashi, M., Rusnák, J., Pinčik, E.: FT IR spectroscopy of silicon oxide layers prepared with perchloric acid, *Appl. Surf. Sci.*, **269**, 106 – 109, (2013).

23 Salmoria, G.V., Leite, J.L., Paggi, R.A.: The microstructural characterization of PA6/PA12 blend specimens fabricated by selective laser sintering. *Pol. Testing*, **28**, [7], 746 – 751, (2009).

24 Karageorgiou, V., Kaplan, D.: Porosity of 3D biomaterial scaffolds and osteogenesis. *Biomater.*, **26**, [27], 5474 – 5491, (2005).

25 Hulbert, S.F., Morrison, S.J., Klawitter, J.J.: Tissue reaction to three ceramics of porous and non-porous structures, *J. Biomed. Mater. Res.*, **6**, [5], 347 – 374, (1972).

26 Hollister, S.J.: Porous scaffold design for tissue engineering, *Nat. Mater.*, **4**, 518 – 524, (2005).

27 Liao, H.T., *et al.*: Fabrication of tissue engineered PCL scaffold by selective laser-sintered machine for osteogenesis of adipose-derived stem cells, *Virtual Phys. Protyp.*, **6**, [1], 57 – 60, (2011).

28 Sudarmadji, N., *et al.*: Investigation of the mechanical properties and porosity relationships in selective laser-sintered polyhedral for functionally graded scaffolds, *Acta Biomater.*, **7**, [2], 530 – 537, (2011).

29 Shuai, C., *et al.*: Optimization of TCP/HAP ratio for better properties of calcium phosphate scaffold via selective laser sintering, *Mater. Charact.*, **77**, 23 – 31, (2013).

30 Yang, S., *et al.*: The design of scaffolds for use in tissue engineering: Part I.: Traditional factors, *Tissue Eng.*, **7**, [6], 679 – 689, (2004).

31 Hao, L., Lawrence, J., Chian, K.S.: Effects of CO_2 laser irradiation on the surface properties of magnesia-partially stabilised zirconia (MgO-PSZ) bioceramic and the subsequent improvements in human osteoblast cell adhesion. *J. Biomater. Appl.*, **19**, 81 – 105, (2004).

32 Hollister, S.J., Maddox, R.D., Taboas, J.M.: Optimal design and fabrication of scaffolds to mimic tissue properties and satisfy biological constraints, *Biomater.*, **23**, [20], 4095 – 4103, (2002).

33 Cowin, S.C.: Bone mechanics handbook, 2nd ed. Boca Raton, CRC Press, 2001.

34 Jameson, J.R.: Characterization of bone material properties and microstructure in osteogenesis imperfecta/brittle bone disease, Marquette University, PhD Thesis, 2014.